Metal–Organic Capsules

International Edition: DOI: 10.1002/anie.201507045
German Edition: DOI: 10.1002/ange.201507045

# An Autocatalytic System of Photooxidation-Driven Substitution Reactions on a $Fe^{II}_4L_6$ Cage Framework

*Prakash P. Neelakandan, Azucena Jiménez, John D. Thoburn, and Jonathan R. Nitschke**

***Abstract:*** *The functions of life are accomplished by systems exhibiting nonlinear kinetics: autocatalysis, in particular, is integral to the signal amplification that allows for biological information processing. Novel synthetic autocatalytic systems provide a foundation for the design of artificial chemical networks capable of carrying out complex functions. Here we report a set of $Fe^{II}_4L_6$ cages containing BODIPY chromophores having tuneable photosensitizing properties. Electron-rich anilines were observed to displace electron-deficient anilines at the dynamic-covalent imine bonds of these cages. When iodoaniline residues were incorporated, heavy-atom effects led to enhanced $^1O_2$ production. The incorporation of (methylthio)aniline residues into a cage allowed for the design of an autocatalytic system: oxidation of the methylthio groups into sulfoxides make them electron-deficient and allows their displacement by iodoanilines, generating a better photocatalyst and accelerating the reaction.*

The development of artificial supramolecular systems capable of complex behavior is a vital strand of current enquiry.[1] Understanding how complexity arises in synthetic systems is helping to elucidate the origins and functioning of life.[2] Processes exhibiting nonlinear kinetics, such as autocatalysis, are central to biological systems[3] and may also form the basis of adaptable materials that respond to environmental stimuli in complex ways.[4]

Metal-ion mediated self-assembly is a fruitful method for the synthesis of complex molecular assemblies.[5] The technique of subcomponent self-assembly utilizes the simultaneous formation of both dynamic covalent (C=N) and coordinative (N→Metal) bonds for the synthesis of three-dimensional structures.[6] Because both coordinative and covalent linkages form reversibly under conditions of thermodynamic equilibration, structures formed using this technique offer more pathways for reconfiguration than do structures held together by a single kind of dynamic linkage. By employing this methodology, we have demonstrated that a variety of metal–organic cage systems can be synthesized and tailored for diverse applications.

We report here a series of $Fe^{II}_4L_6$ cages **1**–**5** (Figure 1), prepared through the reaction of bis(formylpyridyl) BODIPY **L** (where BODIPY is 4,4-difluoro-4-bora-3a,4a-diaza-*s*-indacene) with the anilines $\mathbf{A^1}$–$\mathbf{A^5}$ and iron(II). The identities of the $Fe^{II}_4L_6$ cages were established by one- and two-dimensional NMR and ESI-MS (see Supporting Information, Figures S1–S10). The energy-minimized structures of these cages (Figure S11) were analogous to previously-reported $Fe^{II}_4L_6$ cages derived from linear dialdehyde subcomponents.[7] Their NMR spectra were consistent with *T* point symmetry in solution.

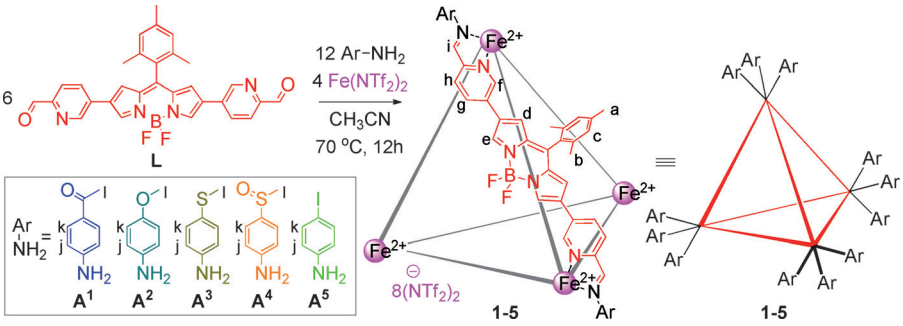


***Figure 1.*** Subcomponent self-assembly of the bis(formylpyridyl)BODIPY **L** with anilines $\mathbf{A^1}$–$\mathbf{A^5}$ and $Fe^{II}(NTf_2)_2$ to form $Fe^{II}_4L_6$ cages **1**–**5**. The structure of only one edge is shown for clarity.

As the BODIPY unit has been shown to be a competent chromophore for the photogeneration of $^1O_2$,[8] we set out to investigate the effects of the substituents of the aniline subcomponents upon $^1O_2$ photogeneration. We thus monitored the ability of cages to generate singlet oxygen by tracking the rate of the reaction of photogenerated $^1O_2$ with 1,3-diphenylisobenzofuran (DPBF), which reacts rapidly with $^1O_2$ (inset of Figure 2).[8d,f] A solution containing both DPBF and cage **5** was exposed to light and UV-Vis absorption spectra were recorded. As shown in Figure 2 and S12, we observed a regular decrease in the absorbance of DPBF as a function of light exposure time, which we attribute to the

[*] Dr. P. P. Neelakandan, Dr. A. Jiménez, Prof. J. R. Nitschke
Department of Chemistry, University of Cambridge
Lensfield Road, Cambridge CB2 1EW (UK)
E-mail: jrn34@cam.ac.uk
Dr. P. P. Neelakandan
Current address: Institute of Nano Science and Technology, Habitat Centre, Phase 10, Sector 64, Mohali 160062 (India)
Dr. A. Jiménez
Current address: Department of Chemistry, University of Oviedo
Julian Clavería 8, Oviedo 33006 (Spain)
Prof. J. D. Thoburn
Department of Chemistry, Randolph-Macon College
Ashland, VA 23005 (USA)

Supporting information for this article is available on the WWW under http://dx.doi.org/10.1002/anie.201507045.

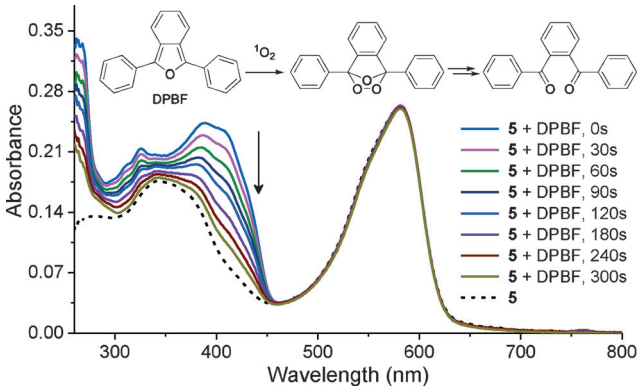


***Figure 2.*** UV-vis spectrum of cage **5** (-----) and the changes in the absorption spectrum of a mixture of cage **5** (1 μM) and DPBF (6.1 μM) in acetonitrile as a function of irradiation time. Inset shows the reaction of singlet oxygen with 1,3-diphenylisobenzofuran (DPBF).

generation of $^1O_2$ photosensitized by cages. At the same time, the absorption bands corresponding to the cages remained unaffected, suggesting the cages to be stable under these conditions. The quantum yields of singlet oxygen generation ($\Phi_\Delta$) were calculated by using methylene blue as a reference of known efficiency.[8d] Cages **1**–**3**, synthesized from non-iodinated anilines, exhibited low $\Phi_\Delta$ values (1–2%), whereas cage **5**, containing iodinated subcomponent $\mathbf{A^5}$, exhibited a higher $\Phi_\Delta = 4.5\,\%$.[9] When a mixture of cage **2** and $\mathbf{A^5}$ was used as photosensitizer, we observed a value of $\Phi_\Delta \approx 2\,\%$, which suggested that the covalent attachment of the iodine-containing species to the BODIPY core is necessary for higher $\Phi_\Delta$.

Although these $\Phi_\Delta$ values are not competitive with established photosensitizers such as methylene blue, the frameworks of these cages are dynamic: electron-rich anilines are capable of displacing electron-poor aniline residues in subcomponent assemblies.[10] We reasoned that the photosensitization efficiency of cages could be tuned via subcomponent exchange, ultimately allowing cages to act as both photosensitizers and substrates for reaction with photogenerated $^1O_2$ in an autocatalytic process. In order to verify this hypothesis, we carried out a transformation in which cage **1** containing electron-poor aniline $\mathbf{A^1}$ (Hammett $\sigma_{para} = 0.50$[11]) and having low $^1O_2$ generation efficiency was transformed into cage **5** by the addition of $\mathbf{A^5}$ ($\sigma_{para} = 0.18$) (Figure 3). Cage **5** thus formed exhibited higher $^1O_2$ generation efficiency than cage **1**. This efficiency was subsequently lowered following exchange of the $\mathbf{A^5}$ residues for more electron-rich non-iodinated aniline $\mathbf{A^2}$ ($\sigma_{para} = -0.27$). Although the singlet oxygen generation efficiency of these cages is modest compared to well-established photosensitizers,[12,13] the dynamic nature of the imine bonds in the cages allows for tuning of the singlet oxygen generation efficiency from an initial low rate to a higher rate, and subsequently back to a lower rate, which would be challenging via conventional methodologies.

We then investigated the consequences of a cage performing dual roles: as both photosensitizer, and as substrate for the photogenerated singlet oxygen. We hypothesized that such

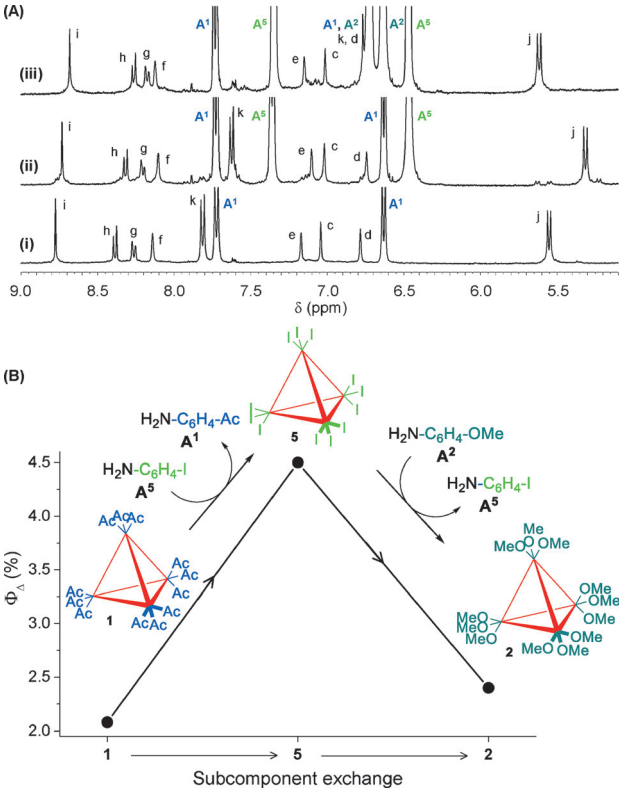


***Figure 3.*** A) Partial $^1$H NMR spectra in $CD_3CN$ of i) cage **1**, ii) cage **5** obtained after addition of $\mathbf{A^5}$ to cage **1**, and iii) cage **2** obtained after addition of $\mathbf{A^2}$ to cage **5**. The resonances corresponding to excess subcomponents $\mathbf{A^1}$, $\mathbf{A^5}$ and $\mathbf{A^2}$ are also labelled. B) Increase in the quantum yield of singlet oxygen generation ($\Phi_\Delta$) upon the conversion of cage **1** into cage **5** after the addition of 4-iodoaniline ($\mathbf{A^5}$), followed by the decrease in $\Phi_\Delta$ upon the conversion of cage **5** into cage **2** after the addition of 4-methoxyaniline ($\mathbf{A^2}$).

a system would exhibit autocatalytic properties: Cage **3** contains 4-(methylthio)aniline ($\mathbf{A^3}$, $\sigma_{para} = 0.0$) residues, which could undergo photooxidation to become electron-deficient 4-(methylsulfinyl)aniline ($\mathbf{A^4}$, $\sigma_{para} = 0.49$) residues (Figure 4).[14] If this reaction were to be carried out in the

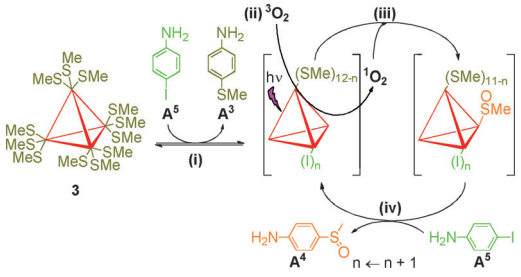


***Figure 4.*** Schematic representation of the autocatalytic photooxidation process that results in accelerating substitution of $\mathbf{A^5}$ for $\mathbf{A^3}$ residues on the framework of **3**. i) Equilibrium subcomponent substitution occurs to a limited degree ($K_{eq} = 0.084$) in the dark. ii) $^3O_2$ is converted into $^1O_2$ more efficiently by cages that contain progressively more $\mathbf{A^5}$ residues as the reaction continues, accelerating it. iii) $^1O_2$ reacts with $\mathbf{A^3}$ residues, converting them into electron-poor $\mathbf{A^4}$ residues, which are then iv) displaced by $\mathbf{A^5}$, increasing by one the number ($n$) of $\mathbf{A^5}$ residues.

  

presence of aniline $\mathbf{A^5}$ ($\sigma_{para} = 0.18$), $\mathbf{A^4}$ would be displaced by the more electron-rich $\mathbf{A^5}$, leading to the generation of cage **5**. Crucially, as this transformation proceeds, the incorporation of progressively more iodinated $\mathbf{A^5}$ residues will increase the photosensitization efficiency of the system, thereby generating more singlet oxygen, which in turn increases the rate of photooxidation of $\mathbf{A^3}$ to $\mathbf{A^4}$. Progressive substitution will thus increase the rate of the photooxidation of the $\mathbf{A^3}$ residues, a behavior characteristic of an autocatalytic system, wherein the rate of reaction accelerates as it progresses.[3]

Figure S13A shows the $^1$H NMR spectrum of cage **3** to which $\mathbf{A^5}$ was added. The reaction medium was then saturated with $O_2$ and exposed to light. After 58 h of illumination, we observed new multiple peaks (mp) overlapping with the $H_j$ and $H_k$ doublets of cage **3** at $\delta = 5.57$ and 7.11 ppm (Figure S13B–E). Concomitantly, new peaks were observed at 5.34 (mp), 6.65 (d) and 7.62 ppm (mp), whose intensity increased at the expense of peaks at 5.57 and 7.11 ppm as the reaction continued. We also observed a small upfield shift ($\Delta\delta = 0.03$) of the signal at 6.65 ppm. As described below, these observations are in accordance with the anticipated photooxidation of cage **3**.

We attribute the appearance of multiple peaks during the course of the reaction to the generation of a dynamic library of cages.[10b] As the photosensitized oxidation proceeds, three kinds of aniline residues are present in the library: $\mathbf{A^3}$ from cage **3**, $\mathbf{A^4}$ from the product of photooxidation, and the added $\mathbf{A^5}$. Six potential bis(iminopyridyl)BODIPY ligands are thus present: three homotopic and three heterotopic, which could form 91 constitutionally distinct cages,[15] leading to the complexity of the observed $^1$H NMR spectra. Chemical shift values of the new peaks at 5.34 and 7.62 ppm were comparable to those of the $H_j$ and $H_k$ protons of cage **5** (Figure S13F), which is consistent with the incorporation of $\mathbf{A^5}$ residues into the cage. Mass spectrometry also supported the presence of a multitude of multiply substituted cage species, containing all three kinds of aniline residues (Figure S14). A complete transformation of the dynamic library into cage **5** was not observed even after prolonged exposure to light and oxygen (13 days at 60 °C).

We tracked the concentration of the displaced aniline $\mathbf{A^3}$ through $^1$H NMR integration as the reaction progressed. As shown in Figure 5 (top trace (▲)), the concentration was observed to increase rapidly during the first ca. 75 h. An intermediate stage was then observed (from ca. 75 h to 250 h), where the rate of substitution was lower. Finally, the rate increased in an exponential fashion after 250 h. We did not observe a final sigmoidal plateau because the NMR peaks broadened, possibly due to a buildup of paramagnetic $Fe^{III}$ produced under oxidizing conditions over several hundred hours.

We infer that the initial rapid release of $\mathbf{A^3}$ is due to an imine exchange reaction that then slows as equilibrium, mostly favoring $\mathbf{A^3}$ incorporation, is reached. The induction period that follows involves photooxidation of $\mathbf{A^3}$ to $\mathbf{A^4}$ followed by release of $\mathbf{A^4}$, slowly at first, and then more rapidly as autocatalysis sets in. The incorporation of iodoaniline ($\mathbf{A^5}$) residues into the cage increases the $^1O_2$ generation efficiency, in turn increasing the rate of the oxidation step.

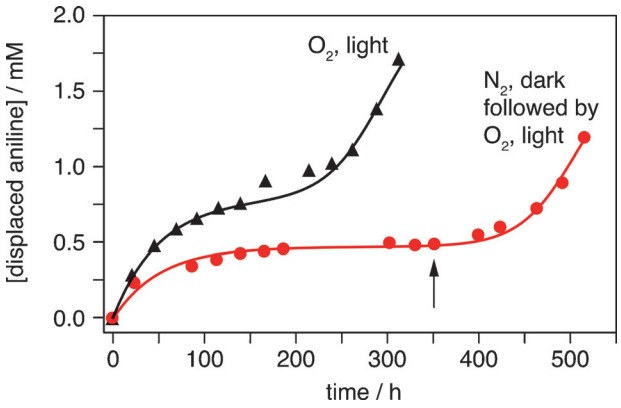


***Figure 5.*** Observed increase in the concentration of the displaced aniline $\mathbf{A^3}$ as a function of time upon irradiating a mixture of cage **3** and $\mathbf{A^5}$ in acetonitrile under different reaction conditions. The arrow indicates the point at which the reaction mixture followed in the lower trace was exposed to $O_2$ and light.

We propose the following set of equations to describe the autocatalytic cycle.[16]

$$\mathbf{5} + {}^3O_2 \rightarrow \mathbf{5} + {}^1O_2 \quad (1)$$

$$\mathbf{3} + {}^1O_2 \rightarrow \mathbf{4} \quad (2)$$

$$\mathbf{4} + \mathbf{A^5} \rightarrow \mathbf{5} + \mathbf{A^4} \quad (3)$$

This system of equations describes an *indirect* autocatalysis, one of the many types of autocatalysis.[17] Oxygen and light participate in the autocatalytic cycle by creating an electron-deficient subcomponent ($\mathbf{A^4}$), the displacement of which becomes thermodynamically favorable during subcomponent substitution. This proposed mechanism is consistent with the kinetic data (See Supporting Information, Section S6 for a detailed analysis).

We carried out a control experiment to test our interpretation of these events, wherein the same transformations were carried out in the absence of light and oxygen (Figure S17). An initial exponential rise in the production of $\mathbf{A^3}$ (Figure 5, lower trace (●)) was observed, with an observed rate constant $k_1^{obs} = 0.018 \pm 0.002\ h^{-1}$, continuing to equilibrium ($K_{eq} = 0.084 \pm 0.002$). However, we did not observe the second exponential rise in the absence of oxygen and light. When the reaction medium was subsequently saturated with oxygen and exposed to light, we observed the characteristic induction period followed by a rapid increase in the rate of the reaction with $k_2^{obs} \approx 45\ M^{-1}h^{-1}$. This control experiment thus supports our hypothesis that photooxidation-driven subcomponent exchange is responsible for autocatalysis.

Comparison of the two experiments of Figure 5 provides further confirmation of autocatalysis: The more rapid initial rise in the rate of substitution in the light reaction (top trace (▲)) as compared to the dark reaction (lower trace (●)) is inferred to be due to the greater degree of incorporation of $\mathbf{A^5}$ residues at earlier times, which engenders a progressively faster substitution rate in the light reaction. If the substitution observed in the light reaction were simply due to a pre-equilibration (as in the dark reaction) followed by displace-

ment of photogenerated $\mathbf{A}^4$ residues, where these residues were being generated at a constant rate, no upward trend in the reaction rate with time would be expected. This observed trend is consistent with a more effective catalyst being generated as more $\mathbf{A}^5$ residues are incorporated.

None of the bis(iminopyridyl)BODIPY cage ligands (Figure 1) were observed to form in the absence of $Fe^{II}$ templates, in keeping with our previous observations that metal templation is required to stabilize the dynamic imine linkages against hydrolysis.[6,7] We thus infer that the cage itself plays an integral role in the autocatalytic system, as any ligand incorporating $\mathbf{A}^5$ residues would hydrolyze rapidly under our experimental conditions in the absence of metal; isolated cage struts appear insufficiently stable to enable the autocatalytic process to proceed.

In summary, by integrating principles of self-assembly and photochemistry, we have demonstrated that the photosensitization efficiency of metal–organic $Fe^{II}_4L_6$ cages could be tuned by subcomponent exchange, which allowed the possibility of post-assembly modification of the cage's structure and reactivity. The ability of the cage to photosensitize singlet oxygen formation can be tuned: substitution with iodoaniline subcomponents enhances the photosensitization, whereas methoxyaniline diminishes it. The singlet oxygen produced was found to oxidize (methylthio)aniline residues, rendering them more readily displaced by iodoaniline, which leads to accelerated photosensitization and an autocatalytic cycle.

Because both a separate molecule (DPBF) and the cage framework itself are able to serve as photooxidation substrates, this cage system might be incorporated into more complex systems. Signal molecules (such as anilines) could be passed to the autocatalytic cycle, enabling the oxidation reaction to be upregulated or downregulated, and the oxidation products themselves could serve as signals to another process. The gearing together of such cycles is an important future direction enabled by this work.

## Acknowledgements

This work was funded by the European Research Council (259352). We thank the NMR service team at the University of Cambridge, Department of Chemistry for help with NMR and the EPSRC Mass Spectrometry Service at Swansea for providing mass spectra.

**Keywords:** autocatalysis · metal–organic capsules · photosensitizers · self-assembly

**How to cite:** *Angew. Chem. Int. Ed.* **2015**, *54*, 14378–14382
*Angew. Chem.* **2015**, *127*, 14586–14590

[1] a) B. Rybtchinski, *ACS Nano* **2011**, *5*, 6791; b) R. Chakrabarty, P. S. Mukherjee, P. J. Stang, *Chem. Rev.* **2011**, *111*, 6810; c) R. S. Forgan, J.-P. Sauvage, J. F. Stoddart, *Chem. Rev.* **2011**, *111*, 5434; d) M. E. Belowich, J. F. Stoddart, *Chem. Soc. Rev.* **2012**, *41*, 2003; e) S. Durot, V. Heitz, A. Sour, J.-P. Sauvage, *Top. Curr. Chem.* **2014**, *354*, 35; f) M. Han, D. M. Engelhard, G. H. Clever, *Chem. Soc. Rev.* **2014**, *43*, 1848; g) Z. He, W. Jiang, C. A. Schalley, *Chem. Soc. Rev.* **2015**, *44*, 779; h) A. Herrmann, *Chem. Soc. Rev.* **2014**, *43*, 1899; i) Q. Ji, R. C. Lirag, O. S. Miljanic, *Chem. Soc. Rev.* **2014**, *43*, 1873; j) T. Le Saux, R. Plasson, L. Jullien, *Chem. Commun.* **2014**, *50*, 6189; k) X. Su, I. Aprahamian, *Chem. Soc. Rev.* **2014**, *43*, 1963; l) A. Wilson, G. Gasparini, S. Matile, *Chem. Soc. Rev.* **2014**, *43*, 1948; m) G. Zhang, M. Mastalerz, *Chem. Soc. Rev.* **2014**, *43*, 1934.

[2] a) G. R. L. Cousins, S.-A. Poulsen, J. K. M. Sanders, *Curr. Opin. Chem. Biol.* **2000**, *4*, 270; b) J.-M. Lehn, *Angew. Chem. Int. Ed.* **2013**, *52*, 2836; *Angew. Chem.* **2013**, *125*, 2906; c) K. Ruiz-Mirazo, C. Briones, A. de La Escosura, *Chem. Rev.* **2014**, *114*, 285.

[3] a) M. Eigen, P. Schuster, *Naturwissenschaften* **1977**, *64*, 541; b) M. Eigen, P. Schuster, *Naturwissenschaften* **1978**, *65*, 7; c) M. Eigen, P. Schuster, *Naturwissenschaften* **1978**, *65*, 341; d) L. E. Orgel, *Nature* **1992**, *358*, 203; e) K. Soai, T. Shibata, I. Sato, *Acc. Chem. Res.* **2000**, *33*, 382; f) K. Soai, T. Kawasaki, A. Matsumoto, *Acc. Chem. Res.* **2014**, *47*, 3643; g) T. Kawasaki, M. Nakaoda, Y. Takahashi, Y. Kanto, N. Kuruhara, K. Hosoi, I. Sato, A. Matsumoto, K. Soai, *Angew. Chem. Int. Ed.* **2014**, *53*, 11199; *Angew. Chem.* **2014**, *126*, 11381; h) K. Severin, D. H. Lee, J. A. Martinez, M. Vieth, M. R. Ghadiri, *Angew. Chem. Int. Ed.* **1998**, *37*, 126; *Angew. Chem.* **1998**, *110*, 133; i) A. J. Bissette, S. P. Fletcher, *Angew. Chem. Int. Ed.* **2013**, *52*, 12800; *Angew. Chem.* **2013**, *125*, 13034; j) Z. Dadon, N. Wagner, S. Alasibi, M. Samiappan, R. Mukherjee, G. Ashkenasy, *Chem. Eur. J.* **2015**, *21*, 648; k) S. Kamioka, D. Ajami, J. Rebek, *Proc. Natl. Acad. Sci. USA* **2010**, *107*, 541.

[4] a) M. Albrecht, *Naturwissenschaften* **2007**, *94*, 951; b) L. Fabbrizzi, *Top. Curr. Chem.* **2012**, *323*, 127; c) A. D. Faulkner, R. A. Kaner, Q. M. A. Abdallah, G. Clarkson, D. J. Fox, P. Gurnani, S. E. Howson, R. M. Phillips, D. I. Roper, D. H. Simpson, P. Scott, *Nat. Chem.* **2014**, *6*, 797; d) G. L. Fiore, S. J. Rowan, C. Weder, *Chem. Soc. Rev.* **2013**, *42*, 7278; e) Y. Inokuma, M. Kawano, M. Fujita, *Nat. Chem.* **2011**, *3*, 349; f) L. A. Joyce, S. H. Shabbir, E. V. Anslyn, *Chem. Soc. Rev.* **2010**, *39*, 3621; g) Y. H. Ko, I. Hwang, D.-W. Lee, K. Kim, *Isr. J. Chem.* **2011**, *51*, 506; h) P. A. Korevaar, T. F. A. de Greef, E. W. Meijer, *Chem. Mater.* **2014**, *26*, 576; i) S. Kubik, *Top. Curr. Chem.* **2012**, *319*, 1; j) M. R. Sambrook, S. Notman, *Chem. Soc. Rev.* **2013**, *42*, 9251; k) L. A. Tatum, X. Su, I. Aprahamian, *Acc. Chem. Res.* **2014**, *47*, 2141; l) S. F. M. van Dongen, S. Cantekin, J. A. A. W. Elemans, A. E. Rowan, R. J. M. Nolte, *Chem. Soc. Rev.* **2014**, *43*, 99; m) C. S. Vogelsberg, M. A. Garcia-Garibay, *Chem. Soc. Rev.* **2012**, *41*, 1892; n) M. D. Ward, P. R. Raithby, *Chem. Soc. Rev.* **2013**, *42*, 1619; o) M. Yoshizawa, J. K. Klosterman, *Chem. Soc. Rev.* **2014**, *43*, 1885.

[5] a) J. J. Becker, M. R. Gagné, *Acc. Chem. Res.* **2004**, *37*, 798; b) J. E. Beves, B. A. Blight, C. J. Campbell, D. A. Leigh, R. T. McBurney, *Angew. Chem. Int. Ed.* **2011**, *50*, 9260; *Angew. Chem.* **2011**, *123*, 9428; c) S. J. Bradberry, A. J. Savyasachi, M. Martinez-Calvo, T. Gunnlaugsson, *Coord. Chem. Rev.* **2014**, *273–274*, 226; d) R. Custelcean, *Chem. Soc. Rev.* **2014**, *43*, 1813; e) G. de Ruiter, M. Lahav, M. E. van der Boom, *Acc. Chem. Res.* **2014**, *47*, 3407; f) M. Mauro, A. Aliprandi, D. Septiadi, N. S. Kehr, L. De Cola, *Chem. Soc. Rev.* **2014**, *43*, 4144; g) S. Mukherjee, P. S. Mukherjee, *Chem. Commun.* **2014**, *50*, 2239; h) K. N. Raymond, C. J. Brown, *Top. Curr. Chem.* **2012**, *323*, 1; i) R. W. Saalfrank, H. Maid, A. Scheurer, *Angew. Chem. Int. Ed.* **2008**, *47*, 8794; *Angew. Chem.* **2008**, *120*, 8924; j) K. Severin, *Chem. Commun.* **2006**, 3859; k) L. Xu, L.-J. Chen, H.-B. Yang, *Chem. Commun.* **2014**, *50*, 5156; l) D. A. Leigh, R. G. Pritchard, A. J. Stephens, *Nat. Chem.* **2014**, *6*, 978.

[6] J. R. Nitschke, *Acc. Chem. Res.* **2007**, *40*, 103.

[7] T. K. Ronson, S. Zarra, S. P. Black, J. R. Nitschke, *Chem. Commun.* **2013**, *49*, 2476.

[8] a) S. Erbas-Cakmak, E. U. Akkaya, *Org. Lett.* **2014**, *16*, 2946; b) S. Lee, R. Stackow, C. S. Foote, A. G. M. Barrett, B. M.

  

Hoffman, *Photochem. Photobiol.* **2003**, *77*, 18; c) R. Göstl, A. Senf, S. Hecht, *Chem. Soc. Rev.* **2014**, *43*, 1982; d) N. Adarsh, M. Shanmugasundaram, R. R. Avirah, D. Ramaiah, *Chem. Eur. J.* **2012**, *18*, 12655; e) A. Kamkaew, S. H. Lim, H. B. Lee, L. V. Kiew, L. Y. Chung, K. Burgess, *Chem. Soc. Rev.* **2013**, *42*, 77; f) C. Zhang, J. Zhao, S. Wu, Z. Wang, W. Wu, J. Ma, S. Guo, L. Huang, *J. Am. Chem. Soc.* **2013**, *135*, 10566; g) J. Zhao, W. Wu, J. Sun, S. Guo, *Chem. Soc. Rev.* **2013**, *42*, 5323.

[9] A further increase in quantum yield was observed for cages synthesized from multi-iodinated anilines. Even though NMR evidence suggested the formation of these cages, mass spectrometry evidence was inconclusive possibly because of fragmentation. Hence we see it inappropriate to include those cages in the manuscript.

[10] a) D.-H. Ren, D. Qiu, C.-Y. Pang, Z. Li, Z.-G. Gu, *Chem. Commun.* **2015**, *51*, 788; b) Y. R. Hristova, M. M. J. Smulders, J. K. Clegg, B. Breiner, J. R. Nitschke, *Chem. Sci.* **2011**, *2*, 638; c) D. Schultz, J. R. Nitschke, *J. Am. Chem. Soc.* **2006**, *128*, 9887.

[11] C. Hansch, A. Leo, R. W. Taft, *Chem. Rev.* **1991**, *91*, 165.

[12] Prior work suggests that the site of iodination is an important factor that governs the efficiency of photosensitization properties of BODIPYs (see Ref. [13]). In cage **5**, the iodine atoms are spatially separated from the BODIPY core, with an $Fe^{II}$ center between them. We infer these factors to reduce the spin–orbit coupling necessary for efficient intersystem crossing, thereby lowering the quantum yields for singlet oxygen generation.

[13] a) M. J. Ortiz, A. R. Agarrabeitia, G. Duran-Sampedro, J. Bañuelos Prieto, T. A. Lopez, W. A. Massad, H. A. Montejano, N. A. García, I. Lopez Arbeloa, *Tetrahedron* **2012**, *68*, 1153; b) T. Yogo, Y. Urano, Y. Ishitsuka, F. Maniwa, T. Nagano, *J. Am. Chem. Soc.* **2005**, *127*, 12162.

[14] L. Wang, J. Cao, J.-w. Wang, Q. Chen, A.-j. Cui, M.-y. He, *RSC Adv.* **2014**, *4*, 14786.

[15] The number of cages that differ in mass was determined as 91 as explained in Ref. [10b].

[16] Equations (1)–(3) are simplified in that **3**, **4**, and **5** are also taken to comprise heteroleptic cages that contain $\mathbf{A^3}$, $\mathbf{A^4}$, and $\mathbf{A^5}$, respectively.

[17] a) R. Plasson, A. Brandenburg, L. Jullien, H. Bersini, *J. Phys. Chem. A* **2011**, *115*, 8073; b) R. Plasson, A. Brandenburg, L. Jullien, H. Bersini, *Artif. Life* **2011**, *17*, 219.

Received: July 29, 2015
Revised: September 15, 2015
Published online: October 6, 2015

  